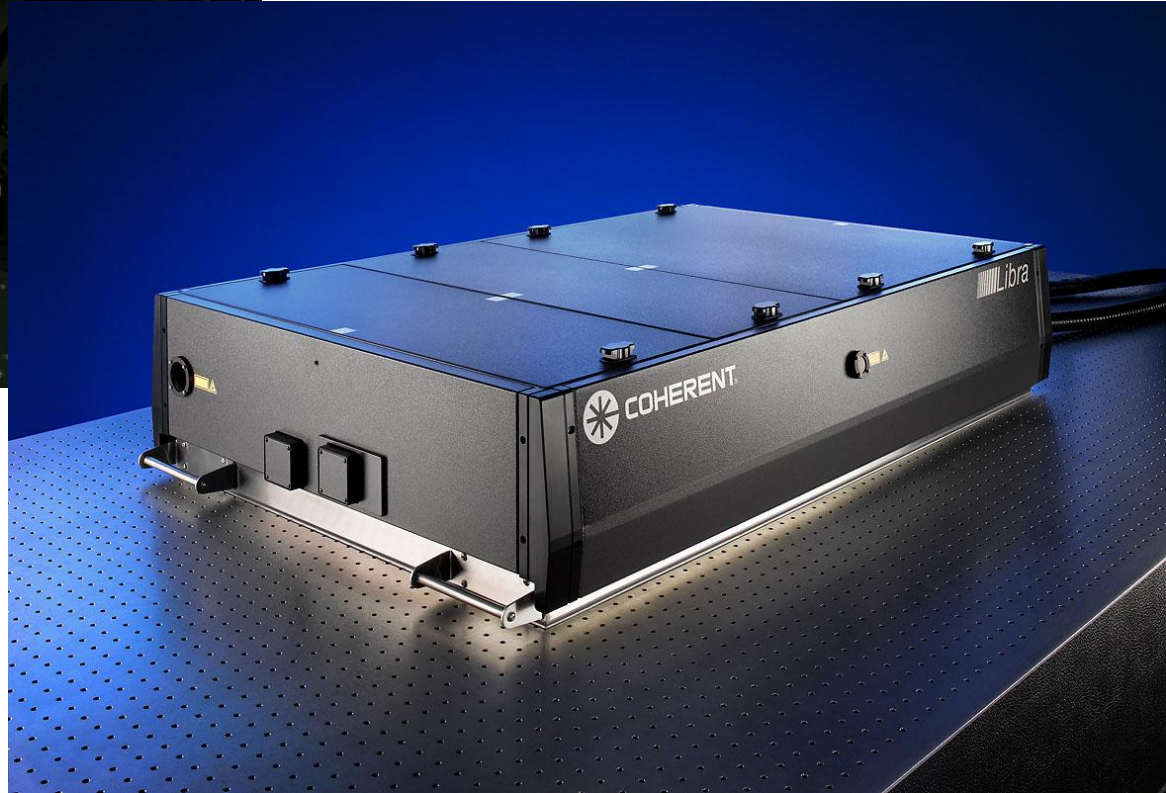


Ti:Sapphire Lasers

: Oscillator, Amplifier



Soft Matter Optical Spectroscopy

Seoncheol Cha

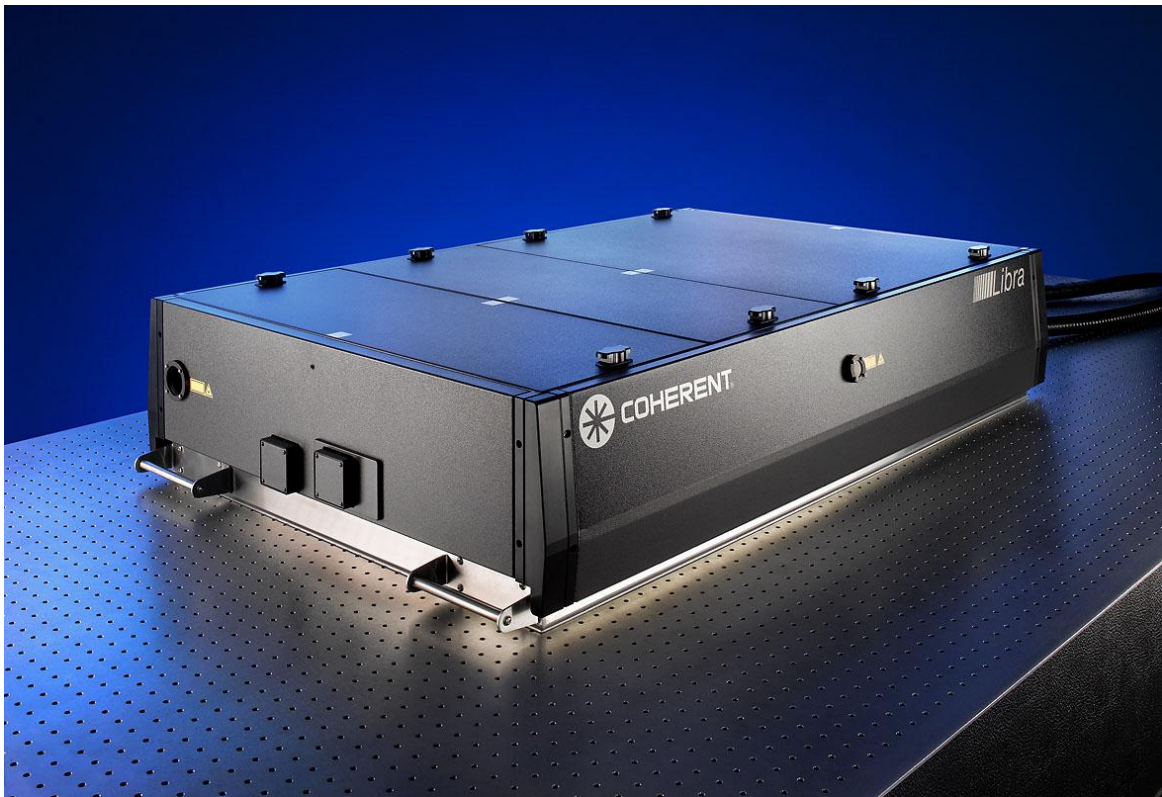
2012.3.24.Sat.

Sum-Frequency Generation Spectroscopy Made by Ti:Sapphire Regenerative Amplifier

Soft Matter Optical Spectroscopy

Seoncheol Cha

2012.6.16.Sat.



Contents

Pump-probe and 2D Sum-Frequency Generation Spectroscopy
Introduction (SFG, Pump-probe spectroscopy)
Setup (Generation of mid-IR, detection)
Results

Phase-sensitive Sum-Frequency Generation Spectroscopy
Concepts & Setup
Analysis
Comparing with conventional SFG
SNR ratio

Femtosecond time-resolved and two-dimensional vibrational sum frequency spectroscopic instrumentation to study structural dynamics at interfaces

Avishek Ghosh, Marc Smits, Jens Bredenbeck, Niels Dijkhuizen, and Mischa Bonn

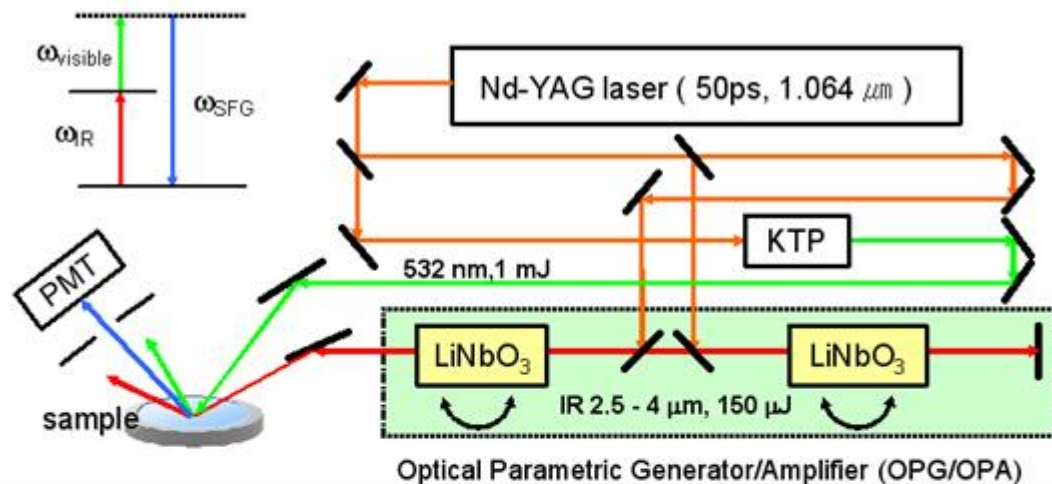
Citation: *Rev. Sci. Instrum.* **79**, 093907 (2008); doi: 10.1063/1.2982058

View online: <http://dx.doi.org/10.1063/1.2982058>

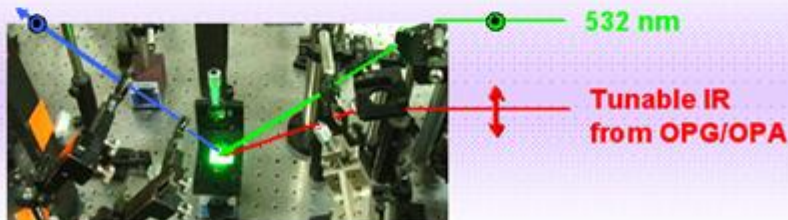
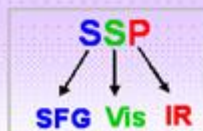
View Table of Contents: <http://rsi.aip.org/resource/1/RSINAK/v79/i9>

Published by the [American Institute of Physics](#).

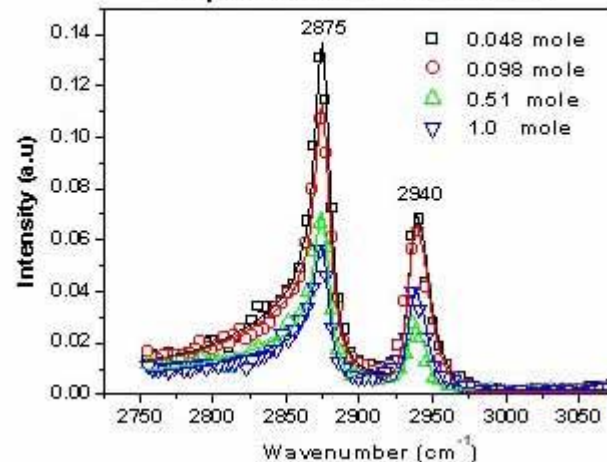
Surface Sum Frequency Generation Spectroscopy



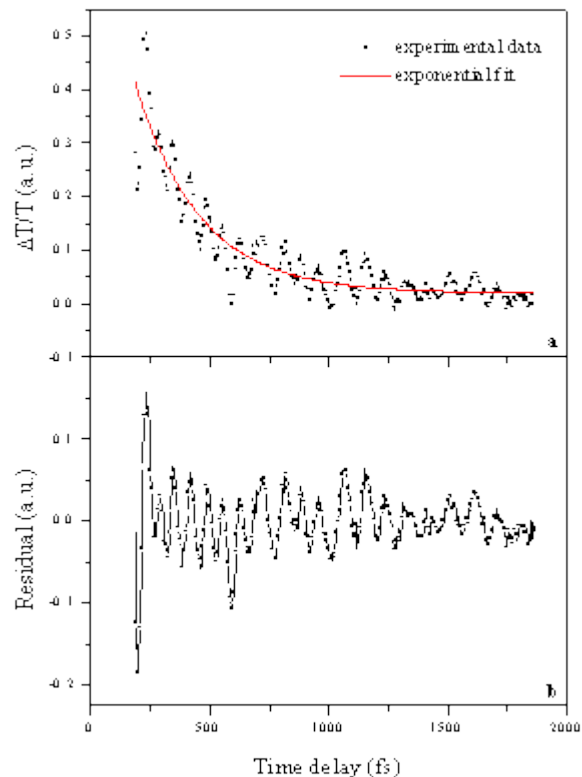
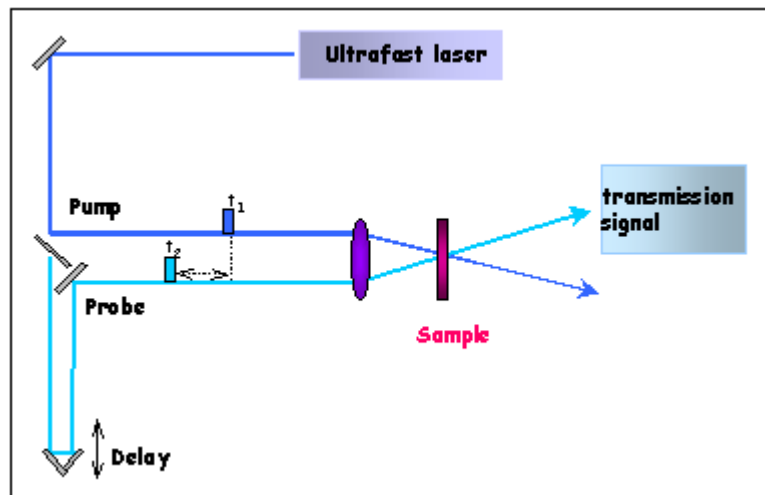
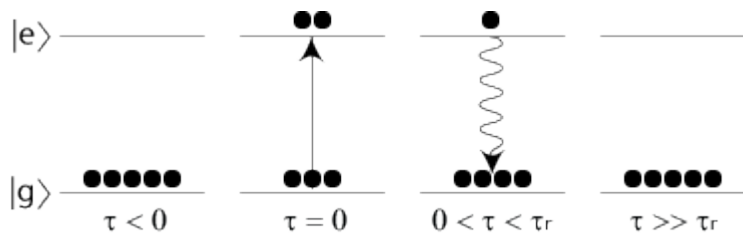
SFG to PMT



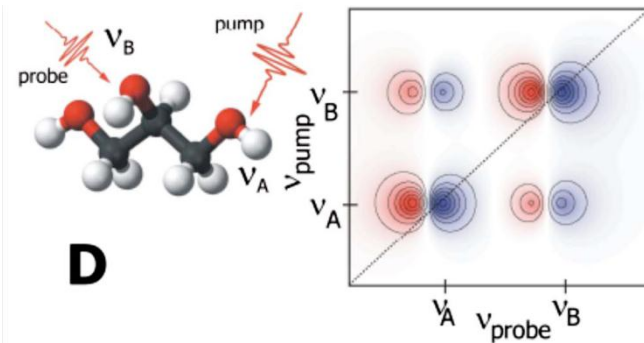
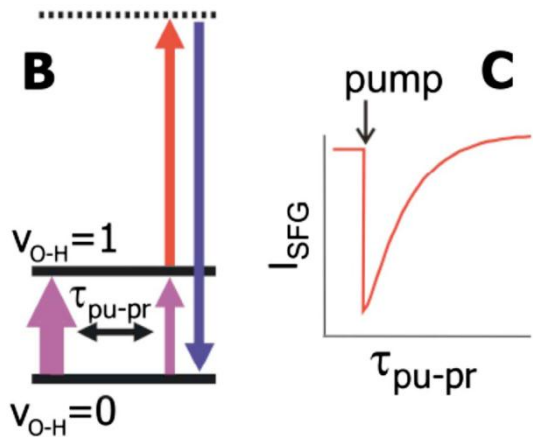
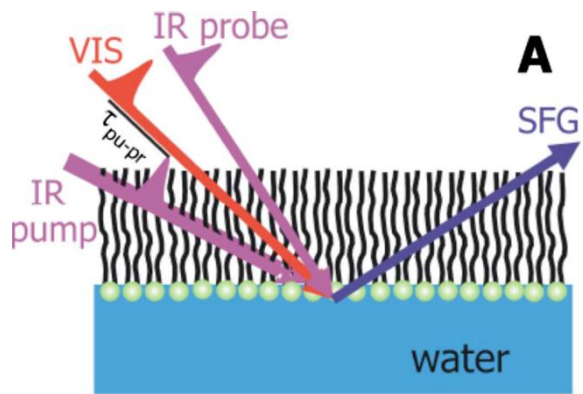
Propanol-water mixture SSP



Pump-Probe Spectroscopy

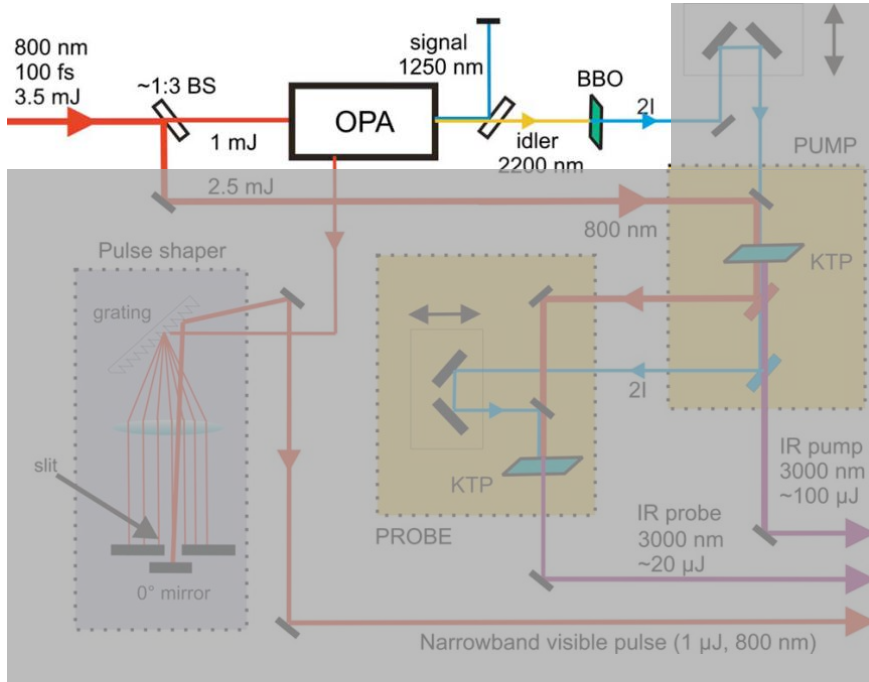


Pump-Probe Surface Sum-Frequency Generation Spectroscopy

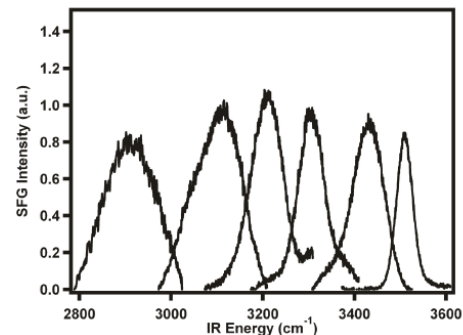
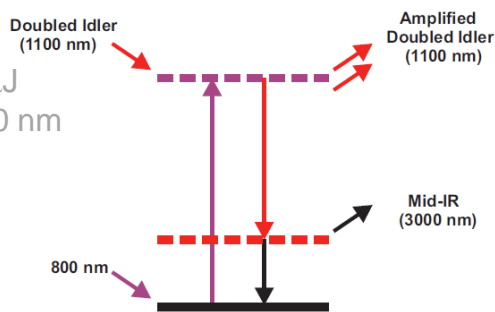
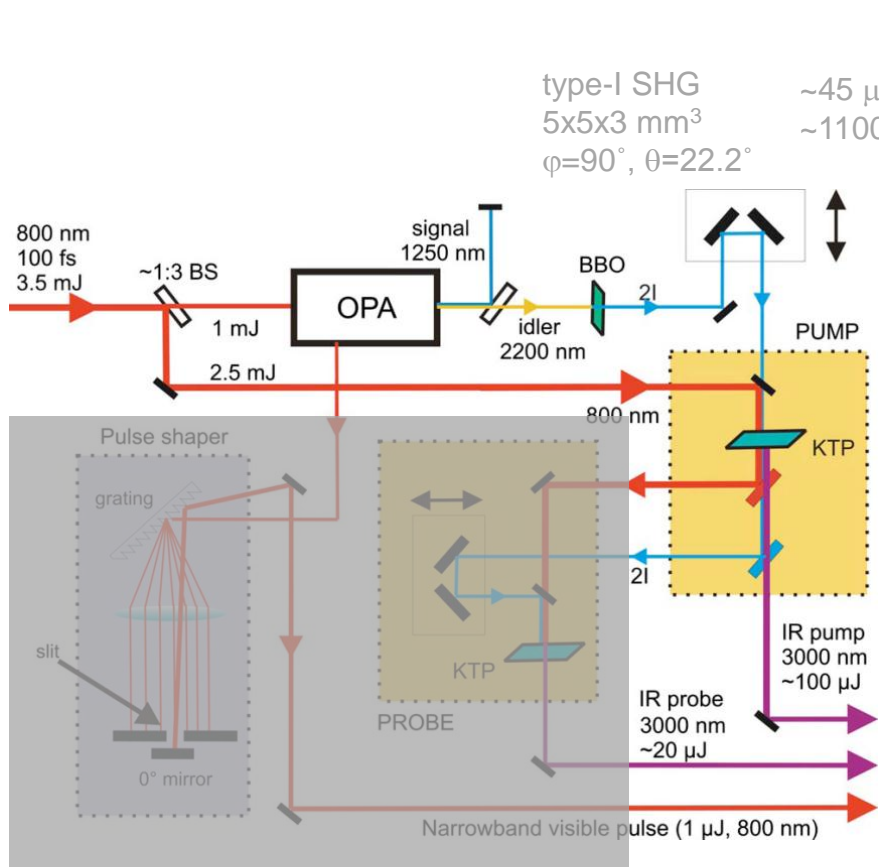


Generation of mid-IR and upconversion pulses

type-I SHG
 $5 \times 5 \times 3 \text{ mm}^3$
 $\varphi = 90^\circ, \theta = 22.2^\circ$
 $\sim 45 \mu\text{J}$
 $\sim 1100 \text{ nm}$

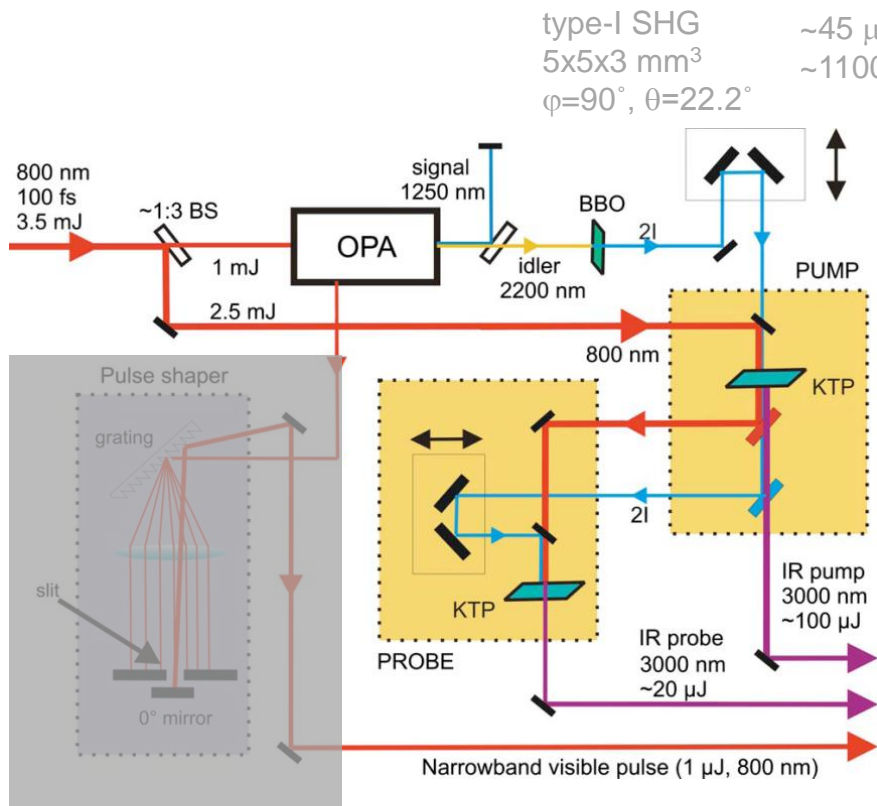


Generation of mid-IR and upconversion pulses



Pump : type II Difference Frequency Mixing
10x10x3 mm³
φ=0°, θ=41.8°
80~100 μJ -> (ND Filter) -> 40 μJ
2860 nm (3496 cm⁻¹) to 3570 nm (2801 cm⁻¹)
FWHM ~ 200cm⁻¹

Generation of mid-IR and upconversion pulses



Pump : type II Difference Frequency Mixing
10x10x3 mm³
φ=0°, θ=41.8°
80~100 μJ → (ND Filter) → 40 μJ
2860 nm (3496 cm⁻¹) to 3570 nm (2801 cm⁻¹)
FWHM ~ 200cm⁻¹

Probe : type II Difference Frequency Mixing (from residual beam)
5x5x3 mm³
φ=0°, θ=41.8°
~25 μJ
FWHM ~ 150cm⁻¹

Probe wavelength can be tuned independently
of the pump wavelength (~ 200 cm⁻¹ detuned)

Generation of mid-IR and upconversion pulses

Pulse shaper

$\text{FWHM}_{\text{input beam}} \sim 12 \text{ nm}$

$\text{FWHM}_{\text{output beam}} \sim 0.6 \text{ nm} (10 \text{ cm}^{-1})$

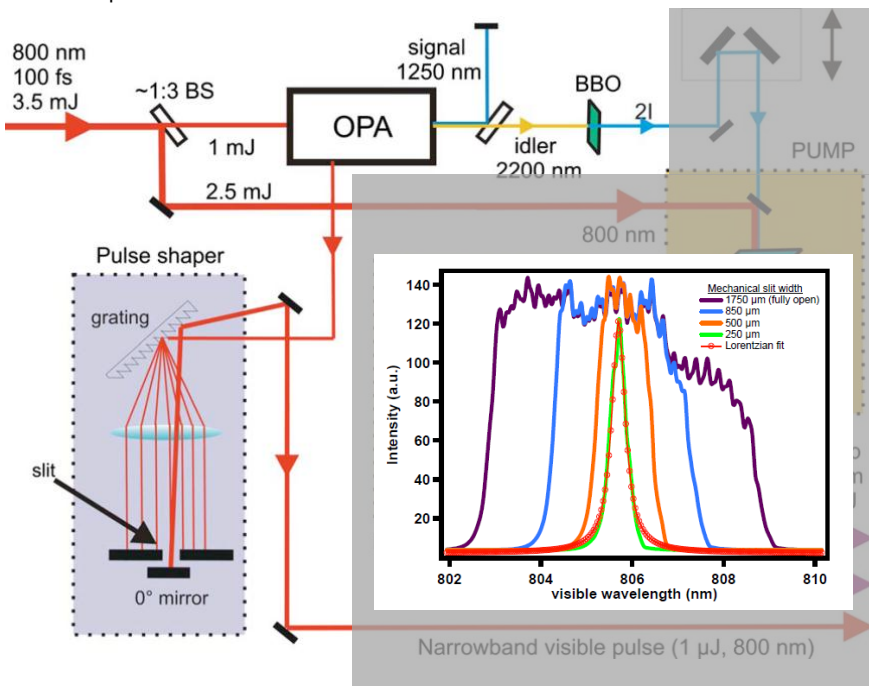
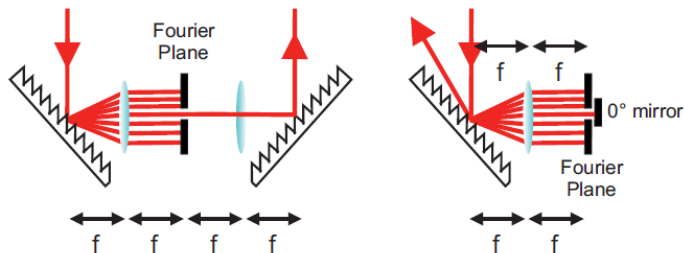
type-I SHG

$5 \times 5 \times 3 \text{ mm}^3$

$\sim 45 \mu\text{J}$

$\sim 1100 \text{ nm}$

$\varphi = 90^\circ, \theta = 22.2^\circ$



Pump : type II Difference Frequency Mixing

$10 \times 10 \times 3 \text{ mm}^3$

$\varphi = 0^\circ, \theta = 41.8^\circ$

$80 \sim 100 \mu\text{J} \rightarrow (\text{ND Filter}) \rightarrow 40 \mu\text{J}$

$2860 \text{ nm} (3496 \text{ cm}^{-1}) \text{ to } 3570 \text{ nm} (2801 \text{ cm}^{-1})$

$\text{FWHM} \sim 200 \text{ cm}^{-1}$

Probe : type II Difference Frequency Mixing (from residual beam)

$5 \times 5 \times 3 \text{ mm}^3$

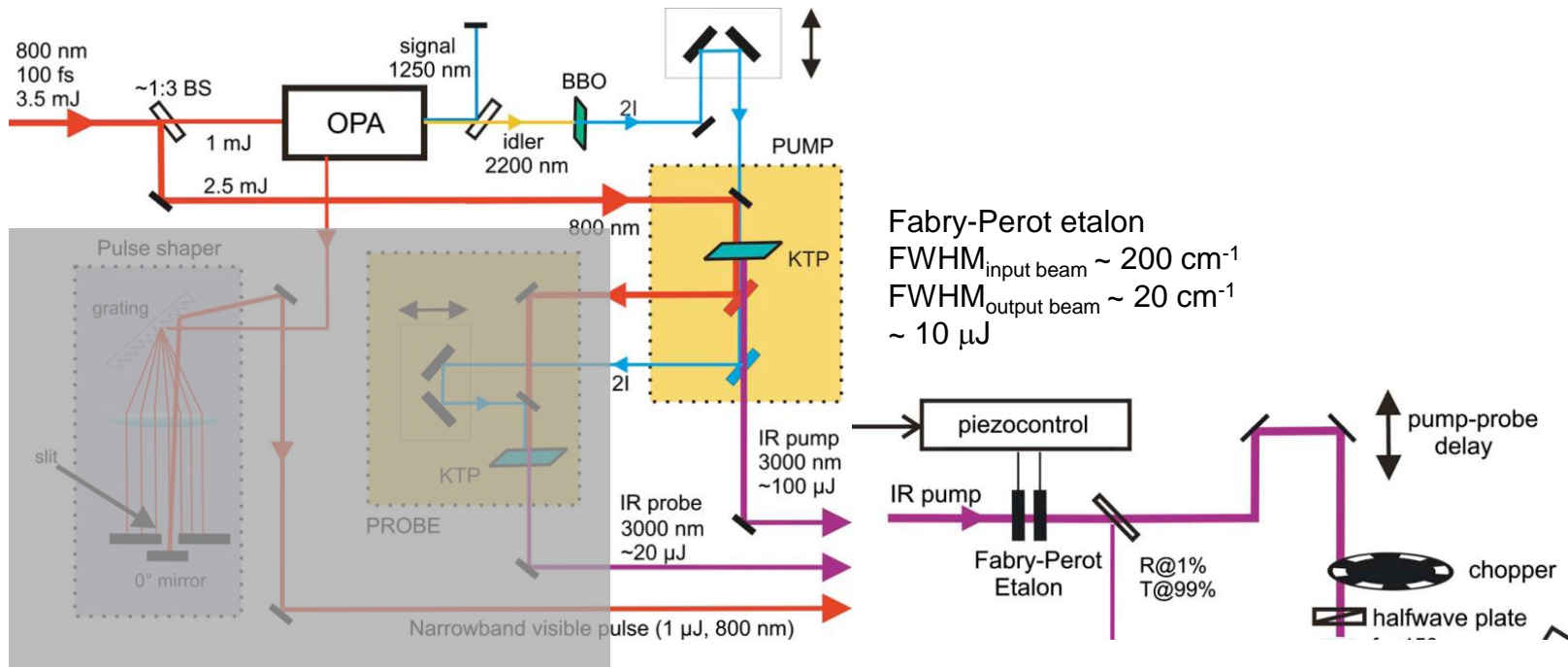
$\varphi = 0^\circ, \theta = 41.8^\circ$

$\sim 25 \mu\text{J}$

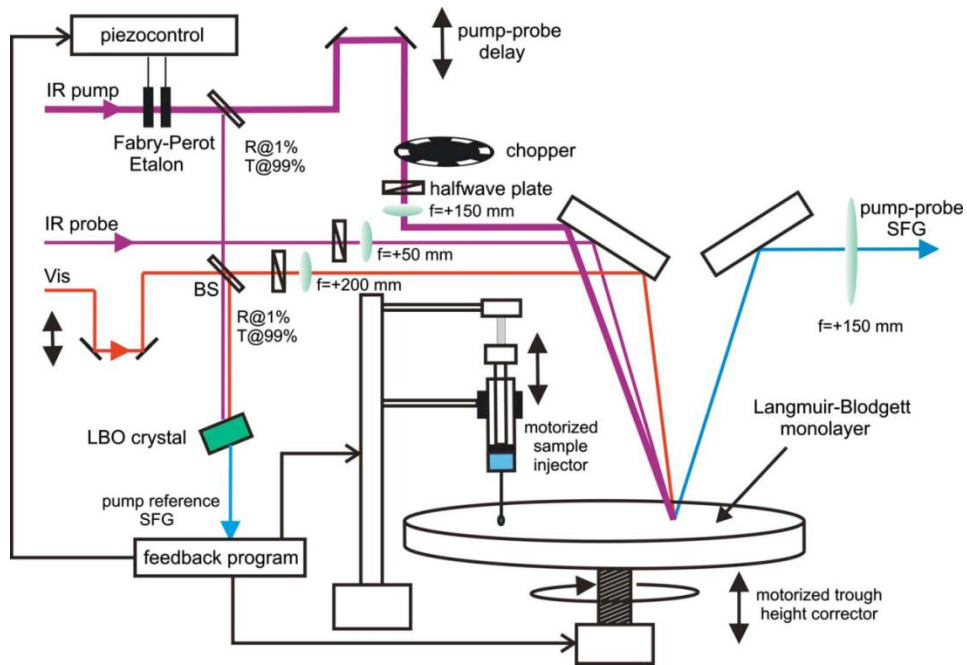
$\text{FWHM} \sim 150 \text{ cm}^{-1}$

Probe wavelength can be tuned independently
of the pump wavelength ($\sim 200 \text{ cm}^{-1}$ detuned)

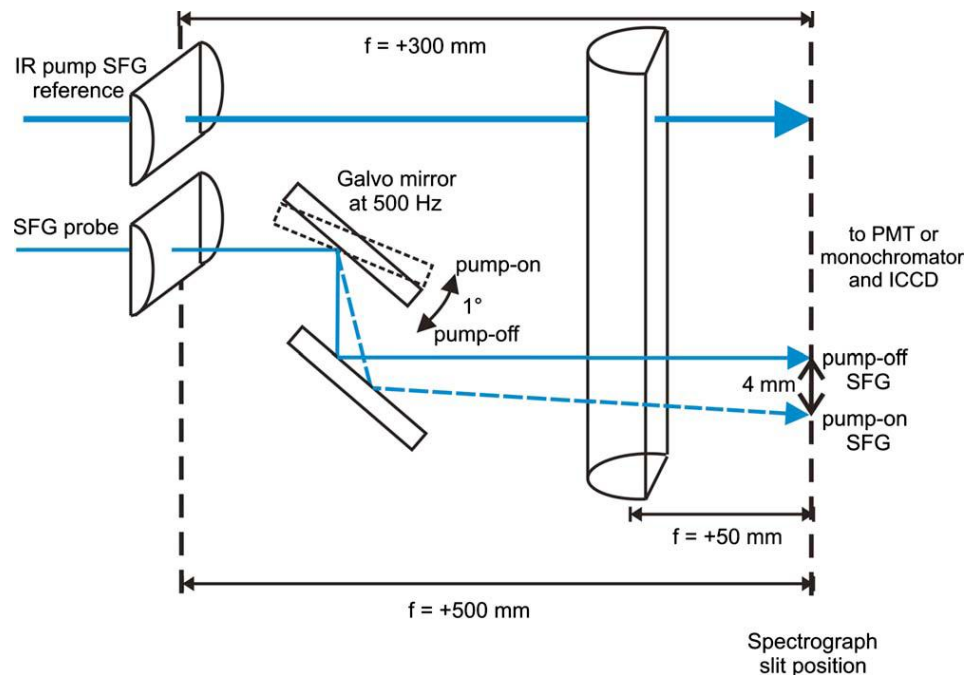
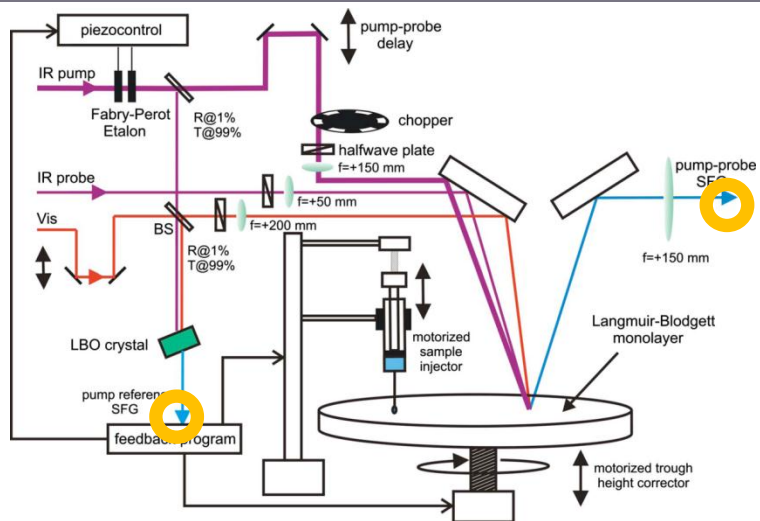
Generation of mid-IR and upconversion pulses for 2D-SFG



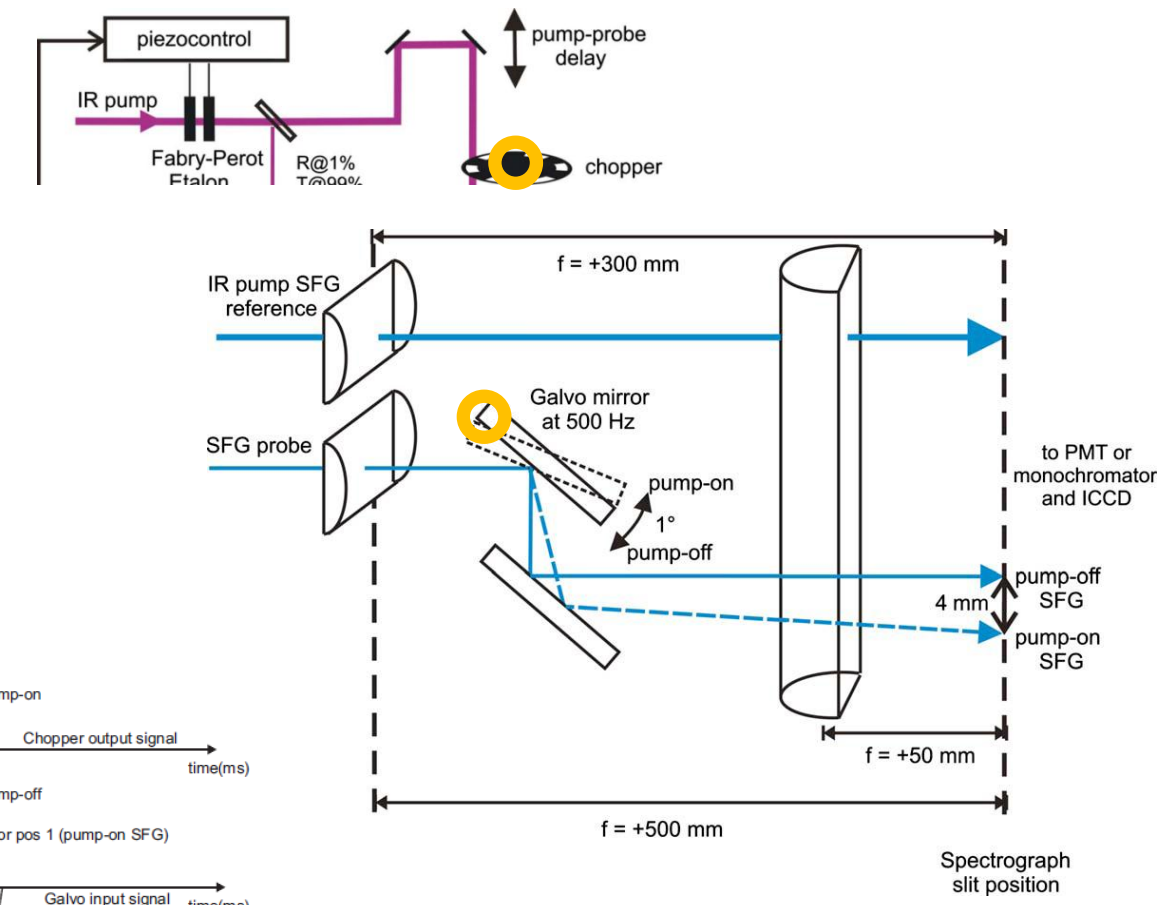
Instrumentation at sample



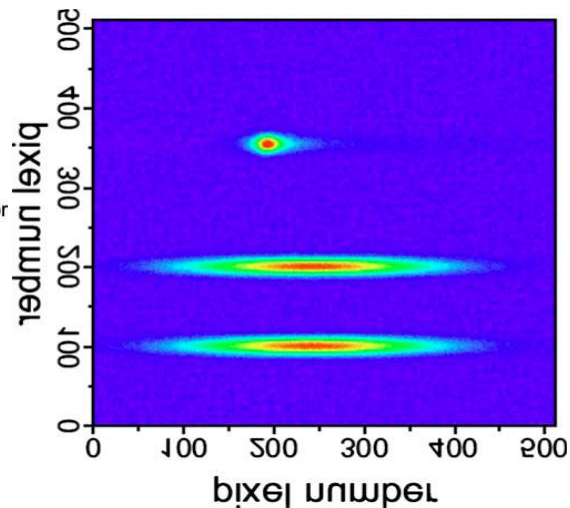
Detection and data acquisition



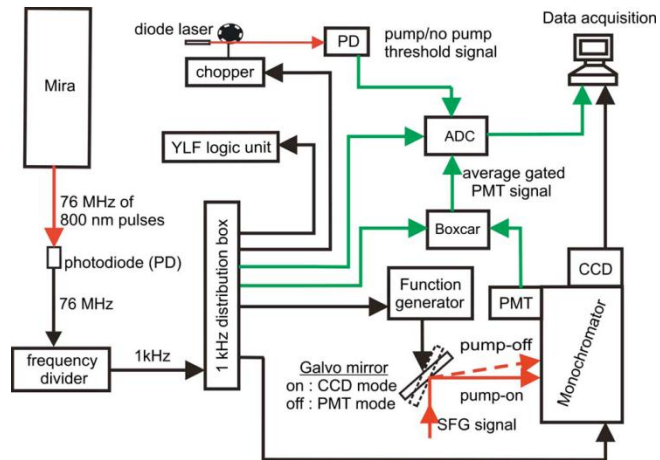
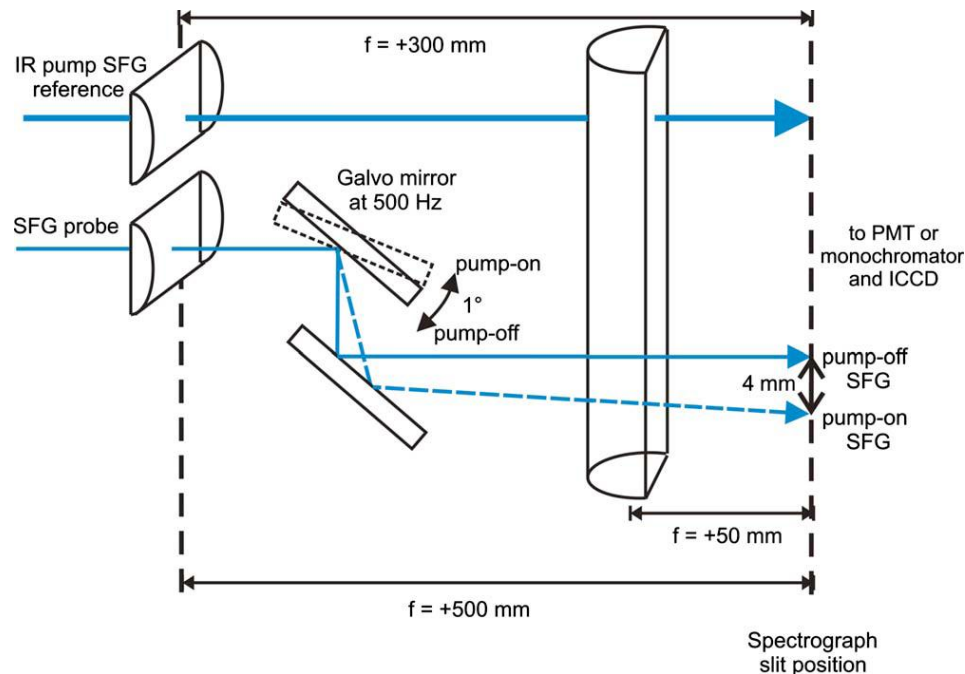
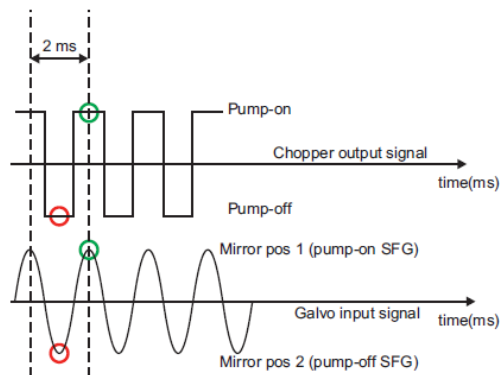
Detection and data acquisition



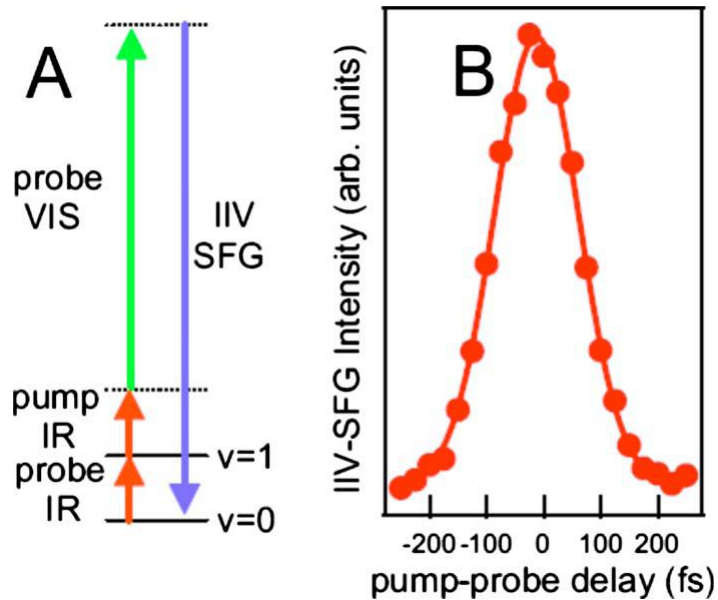
PI iCCD
 512x512 pixels (/24x24 μm)
 < 5nsec, 5 kHz



Detection and data acquisition

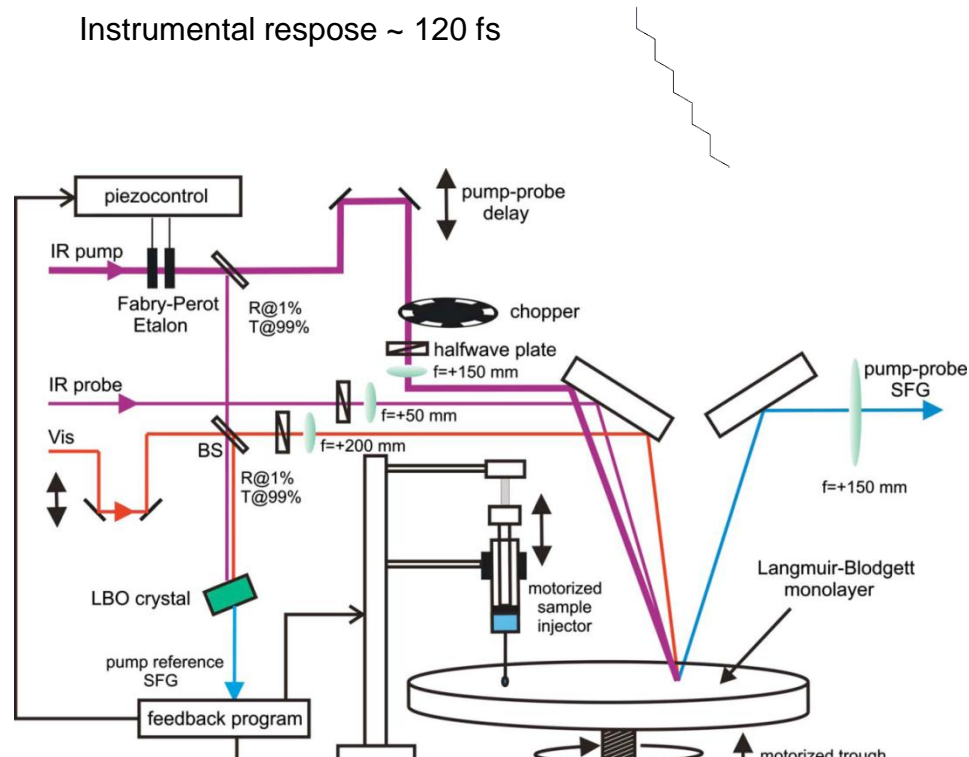


Instrument response



Infrared-infrared-visible Sum-Frequency Generation
at DMPS-water interface

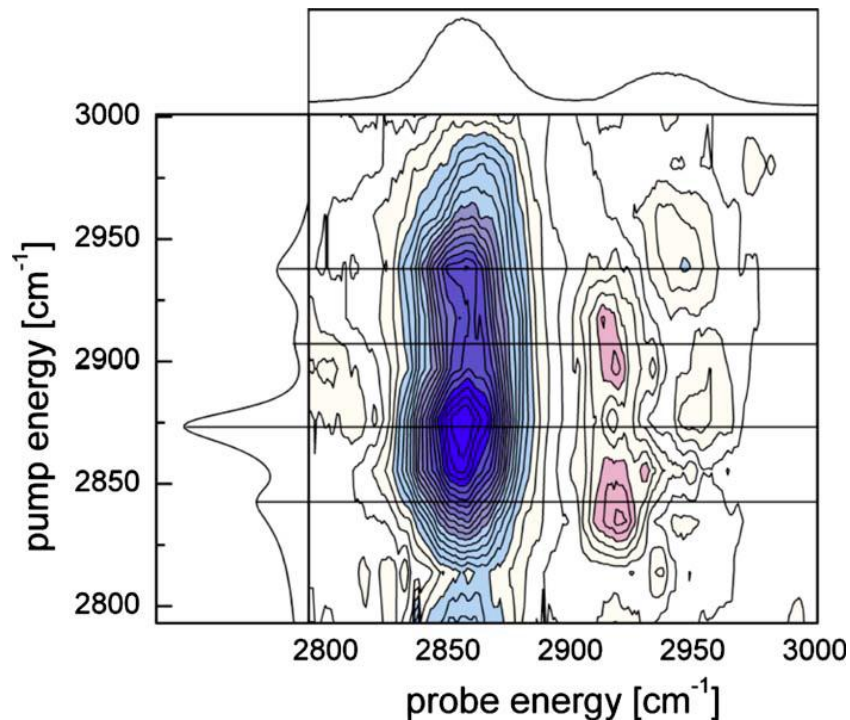
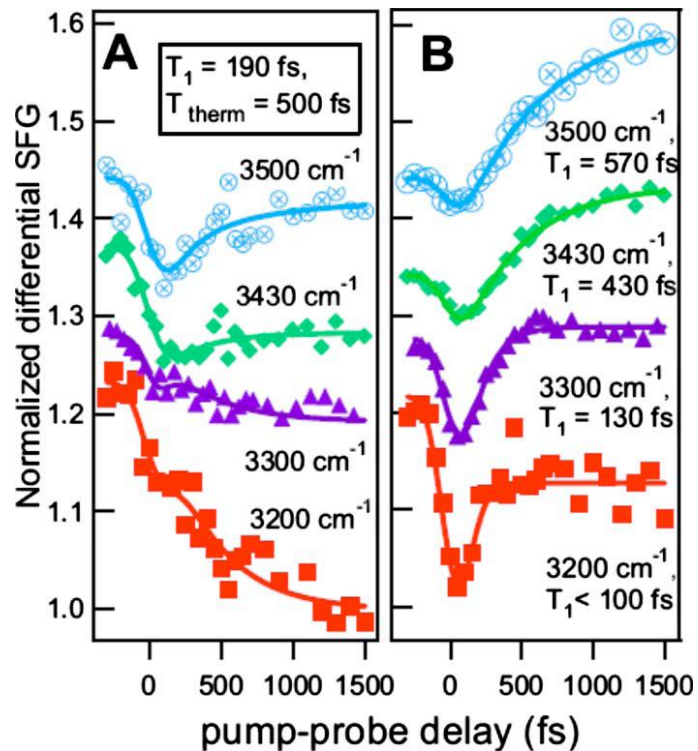
Instrumental response ~ 120 fs



TR-SFG / 2D-SFG results

A : air/water interface

B : air/lipid interface

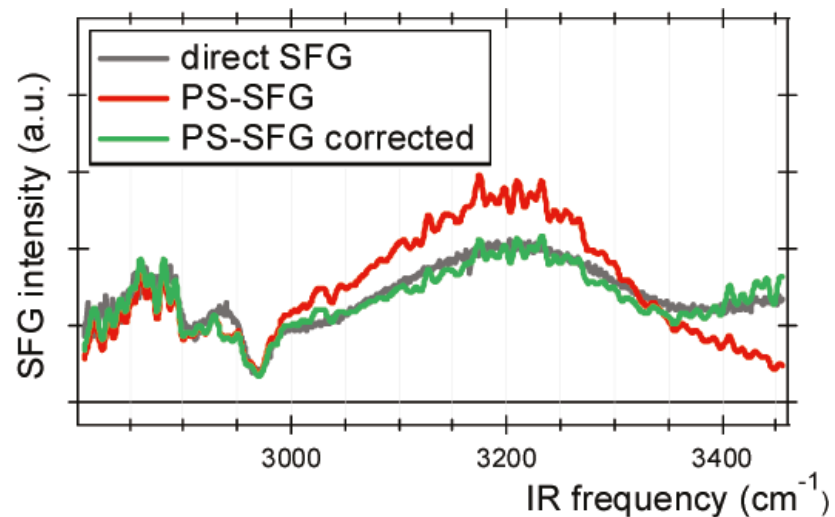
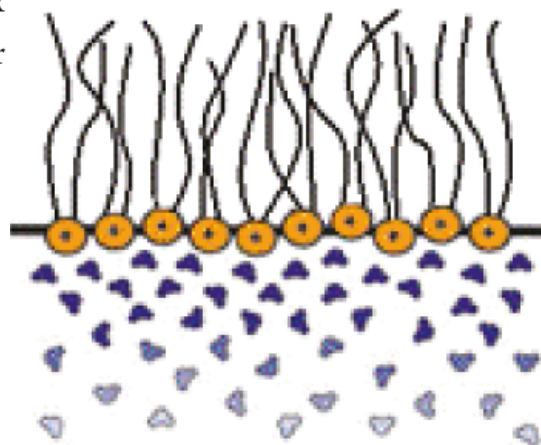


Comparative Study of Direct and Phase-Specific Vibrational Sum-Frequency Generation Spectroscopy: Advantages and Limitations

Ruben E. Pool,[†] Jan Versluis,[†] Ellen H. G. Backus,[†] and Mischa Bonn^{*,†,‡}

[†]Fom Institute AMOLF, P.O. Box

[‡]Max-Planck Institute for Polymer



Direct evidence for orientational flip-flop of water molecules at charged interfaces: A heterodyne-detected vibrational sum frequency generation study

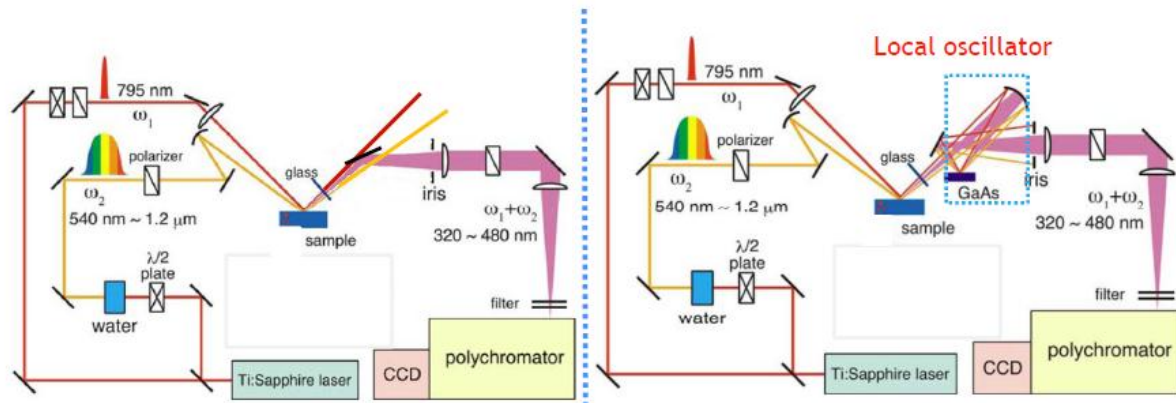
Satoshi Nihonyanagi, Shoichi Yamaguchi, and Tahei Tahara*

(二本柳聡史、山口祥一、田原太平)

Molecular spectroscopy laboratory

Institute (ASI), RIK

2-1 Hirosawa, Wako, Saitama 3



Homodyne detected ESFG spectroscopy

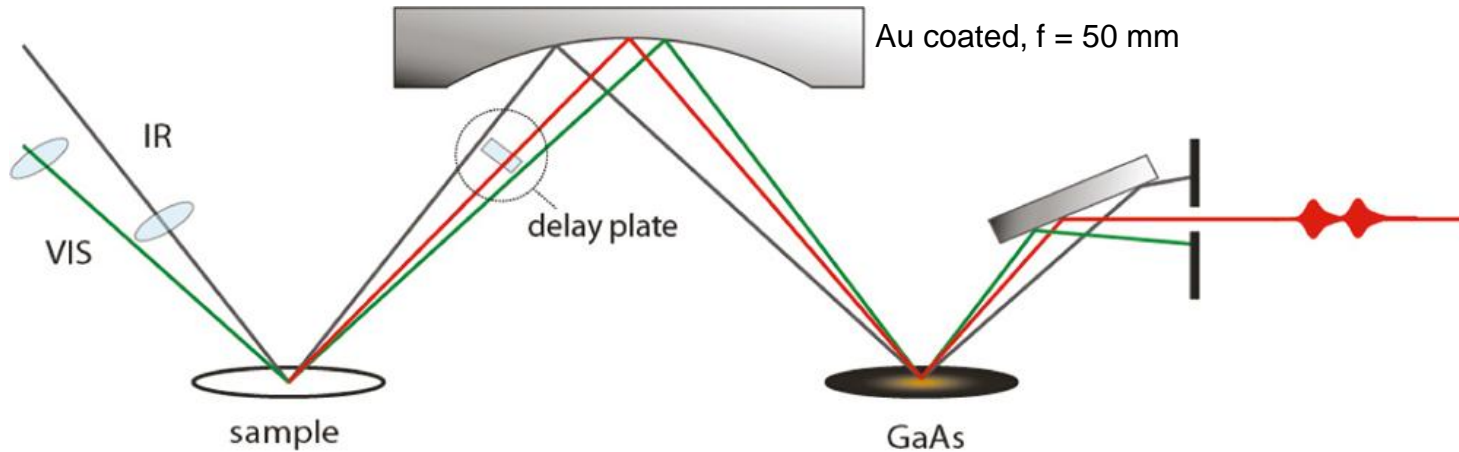
Heterodyne detected ESFG (HD-ESFG) spectroscopy

$$\sim |\chi^{(2)}|^2$$

$$\sim \chi^{(2)} = \text{Re} \chi^{(2)} + \text{Im} \chi^{(2)}$$

\sim absolute orientation (up / down)

Setup



~ 35 fs Ti:Sapphire Sapphire Regenerative Amplifier (Coherent Legend)

1 mJ -> Home made OPA & DFG\

0.5 mJ -> Fabry-Perot etalon -> $\sim 25 \text{ cm}^{-1}$

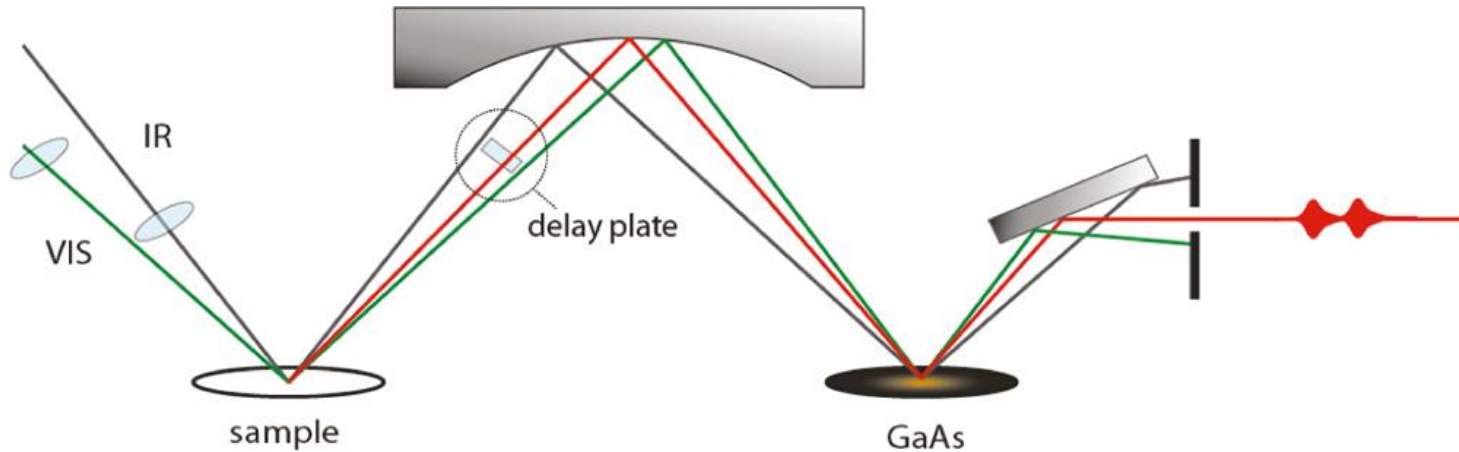
Silica delay plate 1 mm, AR coating

(110) cut GaAs

emCCD

Reflection coefficient of GaAs ~ 0.4
Wavelength independent

Idea of Heterodyne SFG



$$I = |E_{\text{det}}|^2 = |E_{\text{LO}} + E_{\text{sample}}|^2$$
$$= |E_{\text{LO}}|^2 + |E_{\text{sample}}|^2 + E_{\text{LO}} E_{\text{sample}}^* e^{-i\omega\delta t} + E_{\text{LO}}^* E_{\text{sample}} e^{i\omega\delta t}$$

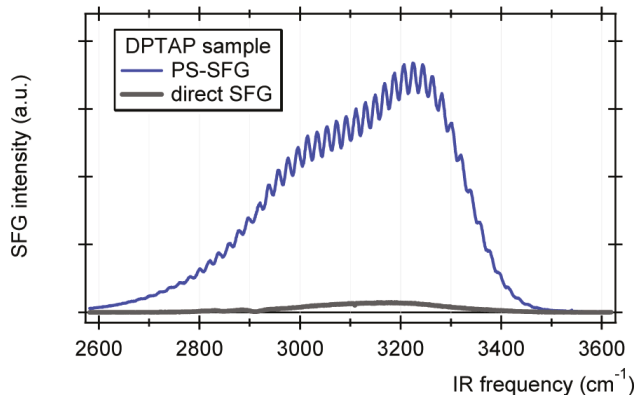
We can obtain interference term \rightarrow phase information (arrangement direction of the molecule)

Fourier Transformation of SFG spectra

Frequency domain

$$E_{\text{det}}(\omega) = E_{\text{LO}}(\omega) + r_{\text{GaAs}}(\omega)E_{\text{sample}}(\omega)e^{i\omega\delta t}$$

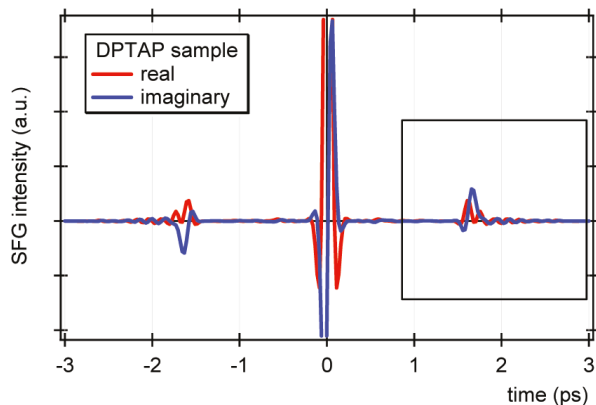
$$I_{\text{det}}(\omega) = |E_{\text{LO}}|^2 + |r_{\text{GaAs}}E_{\text{sample}}|^2 + E_{\text{LO}}r_{\text{GaAs}}E_{\text{sample}}^*e^{-i\omega\delta t} + E_{\text{LO}}^*r_{\text{GaAs}}E_{\text{sample}}e^{i\omega\delta t}$$



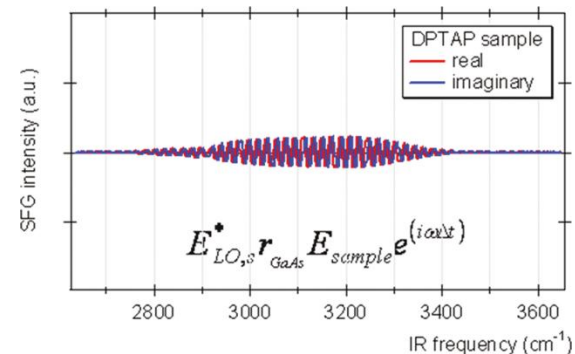
Time domain

$$E_{\text{det}}(t) = E_{\text{LO}}(t) + r_{\text{GaAs}}E_{\text{sample}}(t-\delta t)$$

Pick plus peak only



Frequency domain again



Remark

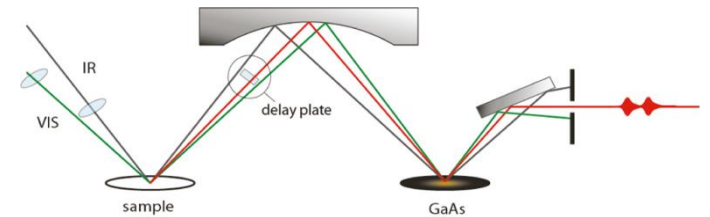
$$I = |E_{\text{det}}|^2 = |E_{\text{LO}} + r_{\text{GaAs}} E_{\text{sample}}|^2$$
$$= |E_{\text{LO}}|^2 + |r_{\text{GaAs}} E_{\text{sample}}|^2 + E_{\text{LO}} r_{\text{GaAs}} E_{\text{sample}}^* e^{-i\omega\delta t} + E_{\text{LO}}^* r_{\text{GaAs}} E_{\text{sample}} e^{i\omega\delta t}$$

$$E_{\text{sample}} = \varepsilon_0 F_{\text{sample}} \chi_{\text{sample}}^{(2)} E_{\text{VIS}} E_{\text{IR}}$$

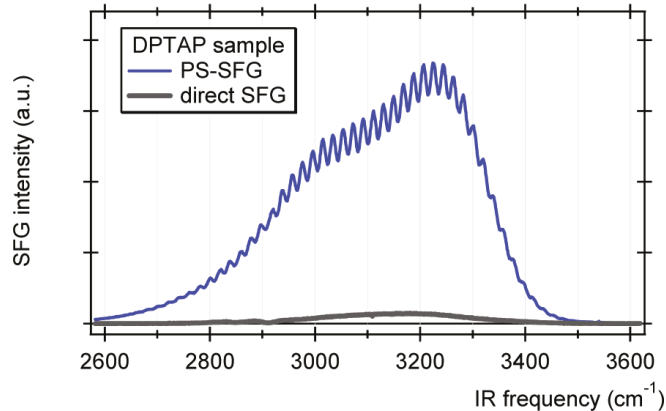
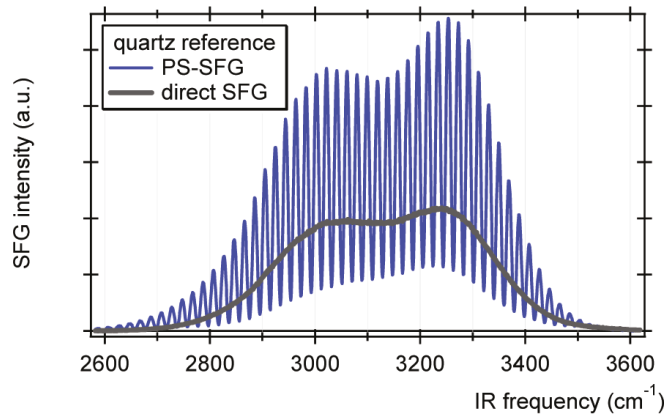
$$E_{\text{LO}} = \varepsilon_0 F_{\text{GaAs}} \chi_{\text{GaAs}}^{(2)} r_{\text{sample}}(\omega_{\text{VIS}}) r_{\text{sample}}(\omega_{\text{IR}}) E_{\text{VIS}} E_{\text{IR}}$$

$E_{\text{LO},s} = E_{\text{LO}}$: generated by GaAs for LO

$E_{\text{LO},q}$: generated by quartz (at sample position)



Normalization of the Phase-Sensitive SFG spectrum



$$I_{PS} \equiv \frac{E_{LO,s}^* r_{GaAs} E_{sample} e^{i\omega\Delta t}}{E_{LO,q}^* r_{GaAs} i E_{quartz} e^{i\omega\Delta t}} = \frac{E_{LO,s}^* E_{sample}}{E_{LO,q}^* i E_{quartz}}$$

i : 90° phase difference between SFG at aqueous interface and quartz is known
[Bloembergen&Pershan PR \(1962\)](#), [Kemnitz et al CPL \(1986\)](#)

$$\begin{aligned} & \frac{E_{LO,s}^* E_{sample}}{i E_{LO,q}^* E_{quartz}} \\ &= \left(\frac{\epsilon_0 F_{GaAs} \chi_{GaAs}^{(2)} r_{sample}(\omega_{VIS}) r_{sample}(\omega_{IR}) E_{VIS} E_{IR}}{\epsilon_0 F_{GaAs} \chi_{GaAs}^{(2)} r_{quartz}(\omega_{VIS}) r_{quartz}(\omega_{IR}) E_{VIS} E_{IR}} \right)^* \frac{\epsilon_0 F_{sample} \chi_{sample}^{(2)} E_{VIS} E_{IR}}{i \epsilon_0 F_{quartz} \chi_{quartz}^{(2)} E_{VIS} E_{IR}} \\ &= \left(\frac{r_{sample}(\omega_{VIS}) r_{sample}(\omega_{IR})}{r_{quartz}(\omega_{VIS}) r_{quartz}(\omega_{IR})} \right)^* \frac{F_{sample} \chi_{sample}^{(2)}}{i F_{quartz} \chi_{quartz}^{(2)}} \end{aligned}$$

$E_{LO,s}$: generated by GaAs for LO

$E_{LO,q}$: generated by quartz (at sample position)

Comparing PS-SFG and Conventional SFG

$$\begin{aligned}
 |I_{\text{PS}}|^2 &= \frac{|E_{\text{LO},s}^* E_{\text{sample}}|^2}{|E_{\text{LO},q}^* E_{\text{quartz}}|^2} = \frac{|r_{\text{sample}}(\omega_{\text{VIS}}) r_{\text{sample}}(\omega_{\text{IR}})|^2 |F_{\text{sample}} \chi_{\text{sample}}^{(2)}|^2}{|r_{\text{quartz}}(\omega_{\text{VIS}}) r_{\text{quartz}}(\omega_{\text{IR}})|^2 |F_{\text{quartz}} \chi_{\text{quartz}}^{(2)}|^2} \\
 &= \frac{E_{\text{LO},s}^* E_{\text{sample}}}{i E_{\text{LO},q}^* E_{\text{quartz}}} \\
 &= \left(\frac{\varepsilon_0 F_{\text{GaAs}} \chi_{\text{GaAs}}^{(2)} r_{\text{sample}}(\omega_{\text{VIS}}) r_{\text{sample}}(\omega_{\text{IR}}) E_{\text{VIS}} E_{\text{IR}}}{\varepsilon_0 F_{\text{GaAs}} \chi_{\text{GaAs}}^{(2)} r_{\text{quartz}}(\omega_{\text{VIS}}) r_{\text{quartz}}(\omega_{\text{IR}}) E_{\text{VIS}} E_{\text{IR}}} \right)^* \frac{\varepsilon_0 F_{\text{sample}} \chi_{\text{sample}}^{(2)} E_{\text{VIS}} E_{\text{IR}}}{i \varepsilon_0 F_{\text{quartz}} \chi_{\text{quartz}}^{(2)} E_{\text{VIS}} E_{\text{IR}}} \\
 &= \left(\frac{r_{\text{sample}}(\omega_{\text{VIS}}) r_{\text{sample}}(\omega_{\text{IR}})}{r_{\text{quartz}}(\omega_{\text{VIS}}) r_{\text{quartz}}(\omega_{\text{IR}})} \right)^* \frac{F_{\text{sample}} \chi_{\text{sample}}^{(2)}}{i F_{\text{quartz}} \chi_{\text{quartz}}^{(2)}} \quad (8)
 \end{aligned}$$

$$I_{\text{direct}} = \frac{|E_{\text{sample}}|^2}{|E_{\text{quartz}}|^2} = \frac{|\varepsilon_0 F_{\text{sample}} \chi_{\text{sample}}^{(2)} E_{\text{VIS}} E_{\text{IR}}|^2}{|\varepsilon_0 F_{\text{quartz}} \chi_{\text{quartz}}^{(2)} E_{\text{VIS}} E_{\text{IR}}|^2} = \frac{|F_{\text{sample}} \chi_{\text{sample}}^{(2)}|^2}{|F_{\text{quartz}} \chi_{\text{quartz}}^{(2)}|^2}$$

Comparing PS-SFG and Conventional SFG

$$|I_{\text{PS}}|^2 = \frac{|E_{\text{LO},s}^* E_{\text{sample}}|^2}{|E_{\text{LO},q}^* E_{\text{quartz}}|^2} = \frac{|r_{\text{sample}}(\omega_{\text{VIS}}) r_{\text{sample}}(\omega_{\text{IR}})|^2 |F_{\text{sample}} \chi_{\text{sample}}^{(2)}|^2}{|r_{\text{quartz}}(\omega_{\text{VIS}}) r_{\text{quartz}}(\omega_{\text{IR}})|^2 |F_{\text{quartz}} \chi_{\text{quartz}}^{(2)}|^2}$$

$$I_{\text{direct}} = \frac{|E_{\text{sample}}|^2}{|E_{\text{quartz}}|^2} = \frac{|\varepsilon_0 F_{\text{sample}} \chi_{\text{sample}}^{(2)} E_{\text{VIS}} E_{\text{IR}}|^2}{|\varepsilon_0 F_{\text{quartz}} \chi_{\text{quartz}}^{(2)} E_{\text{VIS}} E_{\text{IR}}|^2} = \frac{|F_{\text{sample}} \chi_{\text{sample}}^{(2)}|^2}{|F_{\text{quartz}} \chi_{\text{quartz}}^{(2)}|^2}$$

quartz. Since quartz is nonresonant, $\chi_{\text{quartz}}^{(2)}$ is constant (i.e., frequency independent), and $\chi_{\text{sample}}^{(2)}$ can be extracted from this expression by inserting r and F . Traditionally, for direct SFG spectra a correction for F is rarely made, that is, the presented direct SFG spectra are often not corrected for the Fresnel factors; if we proceed with the PS-SFG spectra along the same line, only the reflectivity of the sample and of quartz have to be considered.

$$I_{\text{direct}} = \frac{|F_{\text{sample}} \chi_{\text{sample}}^{(2)}|^2}{|F_{\text{quartz}} \chi_{\text{quartz}}^{(2)}|^2}$$

$$= \frac{|r_{\text{quartz}}(\omega_{\text{VIS}}) r_{\text{quartz}}(\omega_{\text{IR}})|^2}{|r_{\text{sample}}(\omega_{\text{VIS}}) r_{\text{sample}}(\omega_{\text{IR}})|^2} |I_{\text{PS}}|^2 \approx \frac{|r_{\text{quartz}}(\omega_{\text{IR}})|^2}{|r_{\text{sample}}(\omega_{\text{IR}})|^2} |I_{\text{PS}}|^2$$

$r(\omega_{\text{VIS}})$ is roughly frequency independent
Because of narrow bandwidth of VIS pulse

Comparing PS-SFG and Conventional SFG

$$|I_{\text{PS}}|^2 = \frac{|E_{\text{LO},s}^* E_{\text{sample}}|^2}{|E_{\text{LO},q}^* E_{\text{quartz}}|^2} = \frac{|r_{\text{sample}}(\omega_{\text{VIS}}) r_{\text{sample}}(\omega_{\text{IR}})|^2 |F_{\text{sample}} \chi_{\text{sample}}^{(2)}|^2}{|r_{\text{quartz}}(\omega_{\text{VIS}}) r_{\text{quartz}}(\omega_{\text{IR}})|^2 |F_{\text{quartz}} \chi_{\text{quartz}}^{(2)}|^2}$$

$$I_{\text{direct}} = \frac{|E_{\text{sample}}|^2}{|E_{\text{quartz}}|^2} = \frac{|\varepsilon_0 F_{\text{sample}} \chi_{\text{sample}}^{(2)} E_{\text{VIS}} E_{\text{IR}}|^2}{|\varepsilon_0 F_{\text{quartz}} \chi_{\text{quartz}}^{(2)} E_{\text{VIS}} E_{\text{IR}}|^2} = \frac{|F_{\text{sample}} \chi_{\text{sample}}^{(2)}|^2}{|F_{\text{quartz}} \chi_{\text{quartz}}^{(2)}|^2}$$

quartz. Since quartz is nonresonant, $\chi_{\text{quartz}}^{(2)}$ is constant (i.e., frequency independent), and $\chi_{\text{sample}}^{(2)}$ can be extracted from this expression by inserting r and F . Traditionally, for direct SFG spectra a correction for F is rarely made, that is, the presented direct SFG spectra are often not corrected for the Fresnel factors; if we proceed with the PS-SFG spectra along the same line, only the reflectivity of the sample and of quartz have to be considered.

$$I_{\text{direct}} = \frac{|F_{\text{sample}} \chi_{\text{sample}}^{(2)}|^2}{|F_{\text{quartz}} \chi_{\text{quartz}}^{(2)}|^2}$$

$$= \frac{|r_{\text{quartz}}(\omega_{\text{VIS}}) r_{\text{quartz}}(\omega_{\text{IR}})|^2}{|r_{\text{sample}}(\omega_{\text{VIS}}) r_{\text{sample}}(\omega_{\text{IR}})|^2} |I_{\text{PS}}|^2 \approx \frac{|r_{\text{quartz}}(\omega_{\text{IR}})|^2}{|r_{\text{sample}}(\omega_{\text{IR}})|^2} |I_{\text{PS}}|^2$$

$r(\omega_{\text{VIS}})$ is roughly frequency independent
Because of narrow bandwidth of VIS pulse

Comparing PS-SFG and Conventional SFG

$$R_p = \left(\frac{n_1 \cos \vartheta_t - n_2 \cos \vartheta_i}{n_1 \cos \vartheta_t + n_2 \cos \vartheta_i} \right)^2$$
$$= \left(\frac{n_1 \sqrt{1 - \left(\frac{n_1}{n_2} \sin \vartheta_i \right)^2} - n_2 \cos \vartheta_i}{n_1 \sqrt{1 - \left(\frac{n_1}{n_2} \sin \vartheta_i \right)^2} + n_2 \cos \vartheta_i} \right)^2$$

n_1 : index of refraction of air

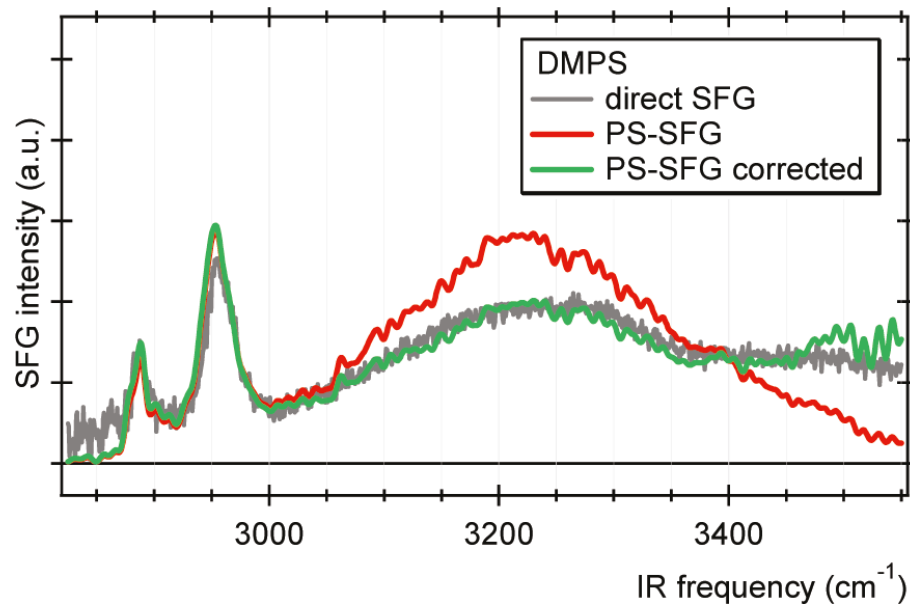
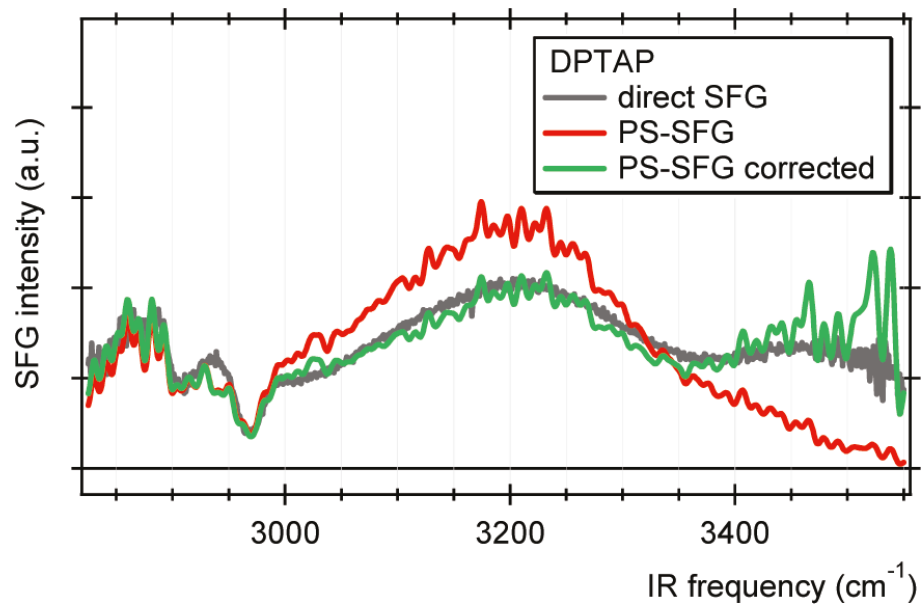
n_2 : index of refraction of water (frequency dependent)

θ_t : angle of refraction

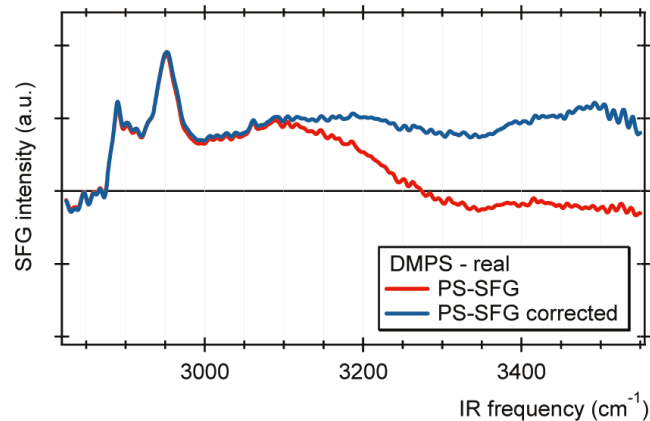
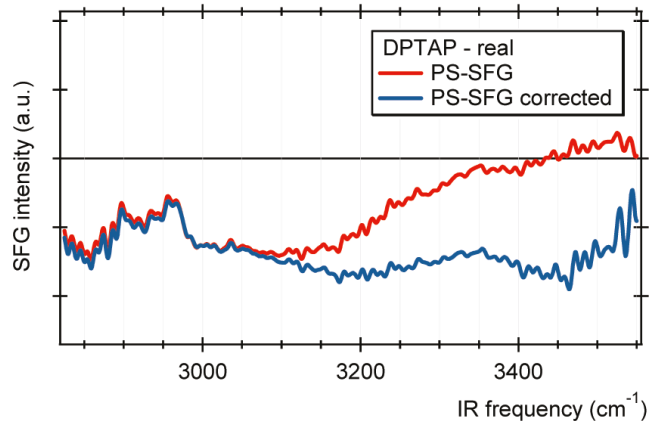
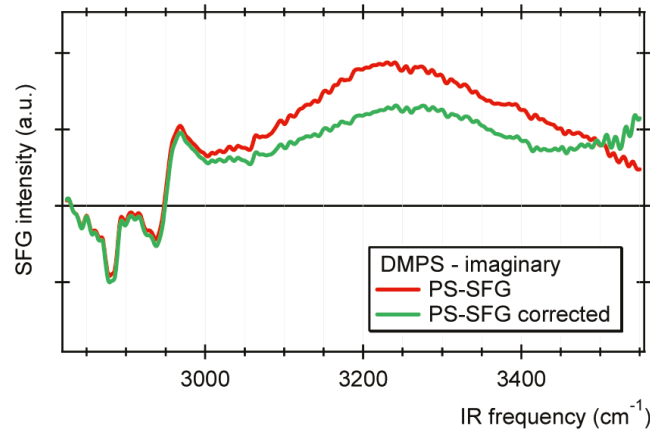
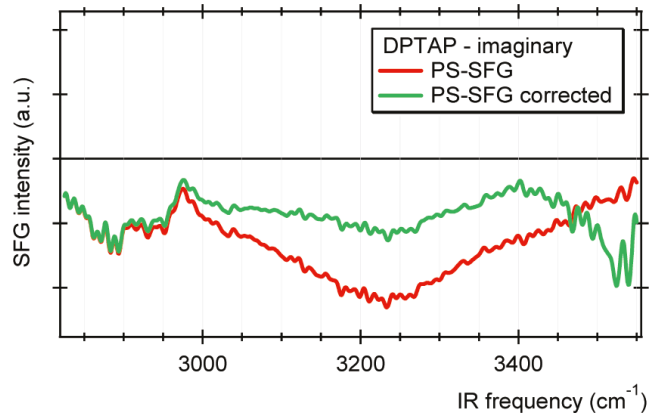
θ_i : angle of incidence w.r.t .surface normal

$$I_{\text{direct}} = \frac{|F_{\text{sample}} \chi_{\text{sample}}^{(2)}|^2}{|F_{\text{quartz}} \chi_{\text{quartz}}^{(2)}|^2}$$
$$= \frac{|r_{\text{quartz}}(\omega_{\text{VIS}}) r_{\text{quartz}}(\omega_{\text{IR}})|^2}{|r_{\text{sample}}(\omega_{\text{VIS}}) r_{\text{sample}}(\omega_{\text{IR}})|^2} |I_{\text{PS}}|^2 \approx \frac{|r_{\text{quartz}}(\omega_{\text{IR}})|^2}{|r_{\text{sample}}(\omega_{\text{IR}})|^2} |I_{\text{PS}}|^2$$

Comparing PS-SFG and Conventional SFG



Correction for PS-SFG at complex spectra



Effect on Phase-Sensitive measurement on Signal to Noise

PS-SFG signal can be orders of magnitude higher than the conventional SFG due to interference with a large SFG signal from LO

Increment of signal-to-noise ratio is reported previously

[Stiopkin *et al*, JACS \(2008\)](#)

[Nihonyanagi *et al*, JCP \(2009\)](#)

[Laaser *et al*, JPCB \(2011\)](#)

[Watanabe *et al*, PRB \(2010\)](#)

$$N_{\text{tot}} = \sqrt{N_{\text{shot}}^2 + N_{\text{DC}}^2 + N_{\text{R}}^2}$$

For deep cooled emCCD

N_{tot} : total noise

N_{shot} : shot noise - 150 to 600 counts / pixel (360s integration at resonance)

N_{DC} : dark current noise ~ 0.002 counts / pixel·second

N_{R} : readout noise ~ 2.8 counts / pixel·readout

Effect on Phase-Sensitive measurement on Signal to Noise

$$\text{SNR}_{\text{direct}} = \frac{I_{\text{sample}}}{N_{\text{tot}}} \approx \frac{I_{\text{sample}}}{N_{\text{shot}}} \propto \frac{I_{\text{sample}}}{\sqrt{I_{\text{sample}}}} = \sqrt{I_{\text{sample}}}$$

$$N_{\text{shot}} > N_{\text{DC}}, N_{\text{R}}$$

$$\text{SNR}_{\text{PS}} = \frac{I_{\text{CT}}}{N_{\text{tot}}} \approx \frac{I_{\text{CT}}}{N_{\text{shot, LO}}} \propto \frac{cI_{\text{sample}}}{cE_{\text{sample}}} = \text{SNR}_{\text{direct}}$$

$$N_{\text{shot}} > N_{\text{DC}}, N_{\text{R}}$$

$$N_{\text{tot}} = \sqrt{N_{\text{shot}}^2 + N_{\text{DC}}^2 + N_{\text{R}}^2}$$

For deep cooled emCCD

N_{tot} : total noise

N_{shot} : shot noise - 150 to 600 counts / pixel (360s integration at resonance)

N_{DC} : dark current noise ~ 0.002 counts / pixel-second

N_{R} : readout noise ~ 2.8 counts / pixel-readout

$$E_{\text{LO}} = cE_{\text{sample}}$$

$$I_{\text{LO}} = c^2 I_{\text{sample}}$$

$$I_{\text{CT}} = E_{\text{LO}} E_{\text{sample}} = cE_{\text{sample}}^2 = cI_{\text{sample}}$$

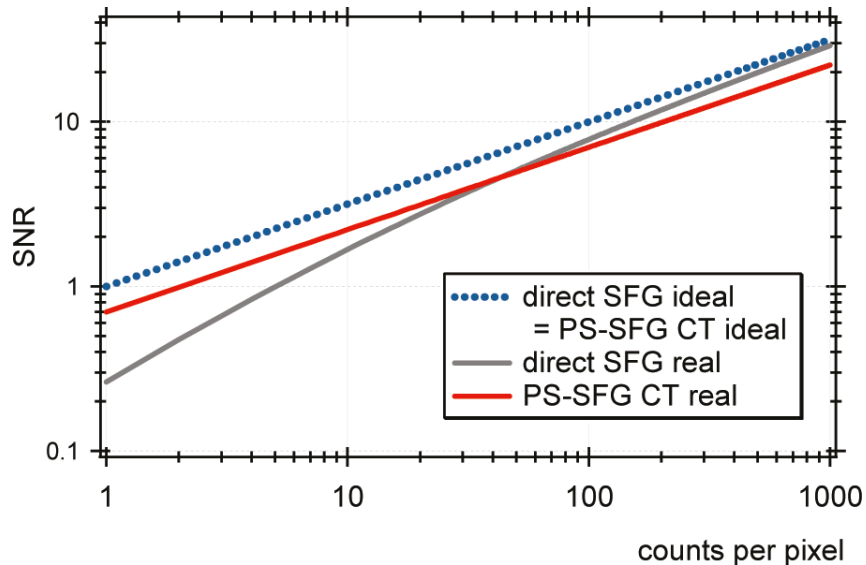
$$N_{\text{shot}} \approx N_{\text{shot, LO}}$$

$$N_{\text{shot, LO}} \propto \sqrt{I_{\text{LO}}} = cE_{\text{sample}} \quad c \gg 1$$

Effect on Phase-Sensitive measurement on Signal to Noise

$$\text{SNR}_{\text{PS}} = \frac{I_{\text{CT}}}{N_{\text{tot}}} \approx \frac{I_{\text{CT}}}{N_{\text{shot, LO}}} \propto \frac{cI_{\text{sample}}}{cE_{\text{sample}}} = \text{SNR}_{\text{direct}}$$

$$N_{\text{shot}} > N_{\text{DC}}, N_{\text{R}}$$



Improvement at low counts / pixel ($N_{\text{DC}}, N_{\text{R}}$ important condition)

Not impressive for high counts / pixel

Real cases : much worse

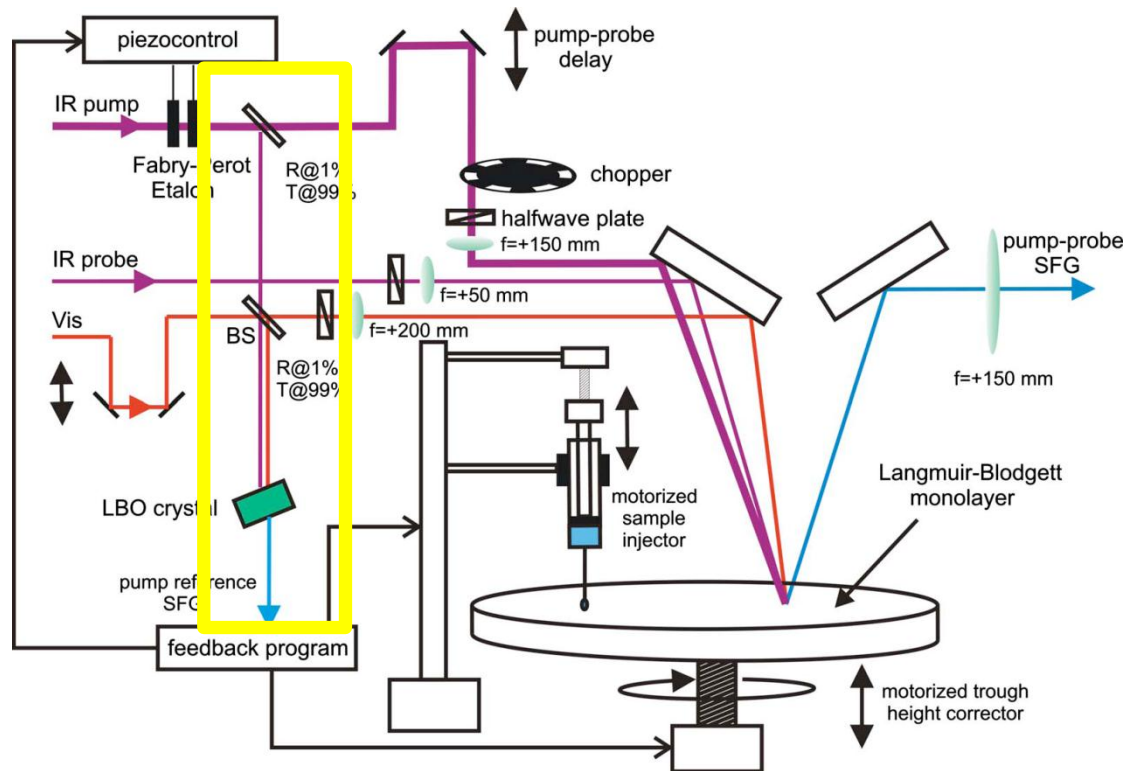
GaAs is not a perfect reflector

Suboptimal interference

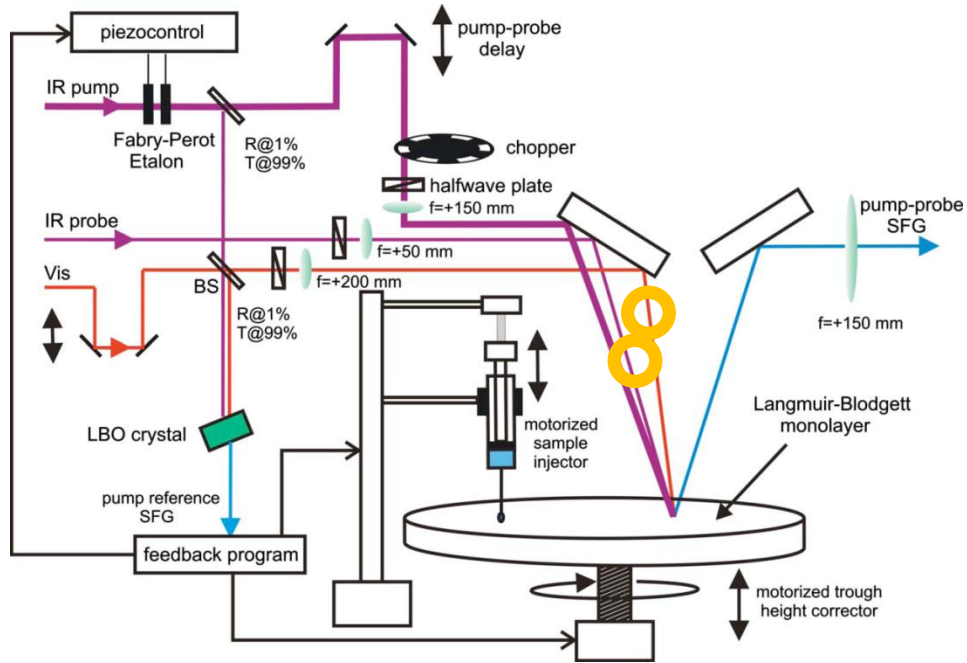
Conclusion

**Time-resolved, 2D, and Phase sensitive SFG measurement
were realized by Ti:S laser**

Calibration excitation frequency

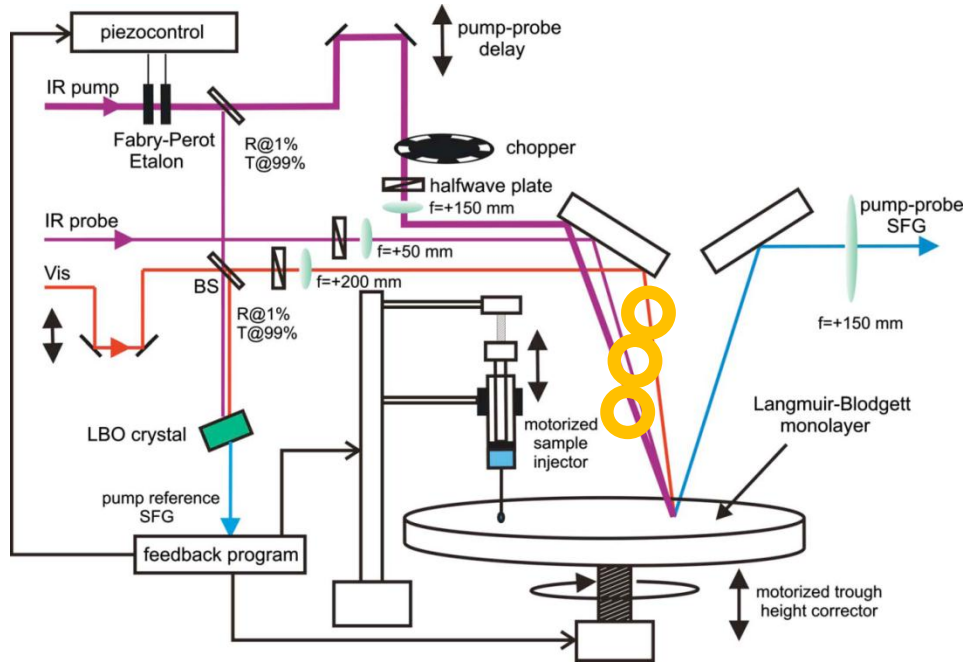


Beam alignment



probe IR beam + visible beam
SFG spectrum at interface
Temporally & spatially overlapped

Beam alignment



probe IR beam + visible beam
SFG spectrum at interface
Temporally & spatially overlapped

probe IR beam + pump IR beam + visible beam
3rd order nonlinear optical process
(infrared-infrared-visible-SFG)

Detection and data acquisition



Andor EMCCD

Good quantum efficiency
Good for air/water
interface

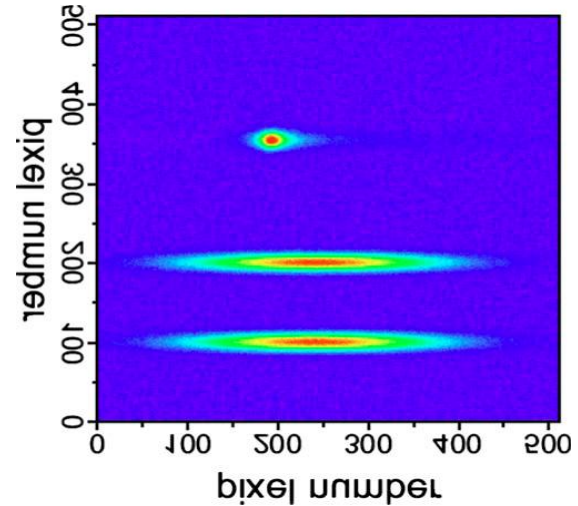


PI iCCD

512x512 pixels (/24x24 μm)
< 5nsec, 5 kHz

Minimal shot noise

Good for lipid/water interface



Software

Software controls the
Pump-probe delay line
Analyzes the CCD images
Trough height modification
Adjustment of the Fabry-Perot piezo voltage

